PHYSICAL REVIEW B VOLUME 21, NUMBER 12 15 JUNE 1980

Optical properties and electronic structure of β'-NiAl

D. J. Peterman, R. Rosei,* and D. W. Lynch
Ames Laboratory, U. S. Department of Energy and Department of Physics, Iowa State University, Ames, Iowa 50011

V. L. Moruzzi
IBM Thomas J. Watson Research Center, Yorktown Heights, New York 10598

(Received 11 February 1980)

The optical constants and their temperature derivatives have been determined for β'-NiAl from absorption and thermoreflectance measurements in the energy range of 0.2–4.4 eV. The results are interpreted using the self-consistent energy bands of Moruzzi, Williams, and Gelatt. By comparing a calculated joint density of states with ϵ_2, the imaginary part of the dielectric function, good overall agreement is found between theory and experiment. In contrast to earlier analyses, it is found that the 2.5-eV peak in ϵ_2 is primarily due to direct interband transitions terminating near the Fermi surface. This new interpretation of the 2.5-eV feature is discussed in relation to previously reported concentration effects and the rigid-band model.

I. INTRODUCTION

Simplifications in the procedures used to calculate the single-particle energy bands of metals[1,2] have made the results of self-consistent energy-band calculations available for many materials. These new calculations, which are becoming more and more accurate due to both the smaller mesh sizes and the stricter self-consistency criteria being employed, allow a detailed comparison between theory and experiment. One experimental technique that lends itself to detailed comparisons with band-structure calculations is thermoreflectance.

The intermetallic compound NiAl was chosen for this study because of its interesting concentration effects. The β'-phase of NiAl exists within the range of 45–60 at.% Ni, making it an excellent material in which one can study the limits of the rigid-band model. Since the number and population of energy states at the Fermi level is affected by temperature as well as species concentration, thermoreflectance experiments can be of use in understanding these concentration effects. Several other groups have studied the electronic structure of β'-NiAl using optical techniques[3-8] and non-self-consistent band-structure calculations.[9-11] As will be seen in the following sections, however, owing to our sensitive optical experiments and the self-consistent band-structure calculations,[12] our understanding of the optical spectra of this alloy is quite different from previous interpretations.

The remainder of this work is organized into three sections. We first discuss briefly the experimental reflectance and thermoreflectance techniques which were employed. Our reflectance results are in agreement with previous results, but, due to our higher sensitivity, reveal more structure. In Sec. III, we detail some of the computational methods used in comparing the band calculations with the optical experiments. Features in the calculated joint density of states are shown to correlate well with the experimentally derived spectra of the imaginary part of the dielectric function $\epsilon_2(\omega)$. In the final section, we discuss the previously reported concentration-dependent optical structure. We examine the rigid-band model and point out some of the pitfalls encountered in using it to interpret peak shifts.

II. EXPERIMENTAL TECHNIQUES AND RESULTS

A near-stoichiometric (50.1 at.% Ni as determined by wet chemical analysis) polycrystalline sample of β'-NiAl was generously provided by F. A. Schmidt of the Ames Laboratory. This was cut into two pieces, one approximately 1 cm × 1 cm × 2 mm for the reflectance study, and the other, $3 \times 3 \times 0.5$ mm^3 for the thermoreflectance work. Both samples were polished in stages ending with 1-μm alumina powder. Immediately prior to being mounted in their respective vacuum chambers, the specimens were electropolished in 6% perchloric acid in methanol at dry ice temperature.

The absorptance ($A = 1 - R$) of NiAl was measured at 4.2 K using a calorimetric technique discussed elsewhere.[13] The advantage of measuring A for metals is that in the infrared, where R approaches unity, an accuracy of 1% in A gives more accuracy for the determination of weak-interband structure than an accuracy of 1% in R. Data were taken in the photon energy range of 0.2 to 4.4 eV. The reflectance spectrum was similar to those shown by other workers,[4,7,8] except for some fine details, and will not be reproduced here. In order to obtain the complex dielectric function, $\tilde{\epsilon} = \epsilon_1 - i\epsilon_2$, Kramers-Kronig integrals were carried out. The extrapolations used were the following: a Drude term below 0.2 eV, data of Kiewit *et al.*[4] from 4.4 to 5.6 eV, a shifted average of Ni (Ref. 14) and

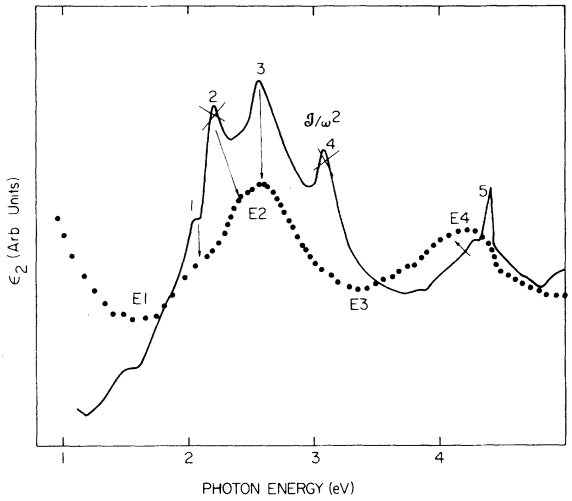

FIG. 1. $\epsilon_2(\omega)$ from absorbance measurements (dotted line) and $\mathcal{J}(\omega)/\omega^2$ from JDOS calculations (solid line). The $\vec{k}$-space origin of the numbered theoretical features is summarized in Table I and discussed in relation to experimental structure. The arrows connect features in the calculations with the appropriate experimentally observed features in $\epsilon_2(\omega)$ and the ×'s indicate transitions not allowed by symmetry on symmetry lines.

Al (Ref. 15) optical data from 5.6 to 27 eV, and a power-law function from 27 to 5000 eV.

The ϵ_2 spectrum is shown as a dotted line in Fig. 1. The effect of using an inaccurate extrapolation on this curve would be to modify peak heights slightly, but it is the shape of the spectrum which is of most interest to us. Compared to other experimental results for ϵ_2, ours displays a bit more structure in the first gross peak labeled $E2$. There is a shoulder near 2.1 eV and evidence of peaks at 2.40 and 2.60 eV. Rechtien *et al.*[5] also had a slight shoulder near 2.1 eV but only a broad, structureless peak at 2.5 eV. The second major feature, labeled $E4$ in Fig. 1, is less symmetric in our work with a shoulder evident on the low-energy side. Before comparing these features with band-structure calculations, we look at our thermoreflectance results.

The thermoreflectance of NiAl was measured at near-normal incidence between 0.5 and 5 eV using PbS and photomultiplier detectors. The sample was glued, using Duco cement diluted with acetone, to a Cr-film heater on a sapphire substrate. This assembly was then placed in a cryostat using liquid nitrogen as coolant. A unipolar 2-Hz square wave with an average power of 7 W passed through the heater, bringing the sample temperature up to about 145 K. The temperature amplitude of modulation was 1–3 K and conventional lock-in techniques were used to measure $\Delta R/R$.[16] For the Kramers-Kronig analysis, the extrapolation of $\Delta R/R$ to high and low energies to get $\Delta\tilde{\epsilon}$ is not as critical as the extrapolation of R to get $\tilde{\epsilon}$.[17] The low-energy limit was fitted to a temperature-modulated Drude term and the high-energy side was extended smoothly to zero.

The $\Delta\epsilon_2$ spectrum is shown in Fig. 2 as a dotted line. As can be seen, there is one major feature which is antisymmetric about 2.40 eV with smaller, similar structures at 1.80 and 3.95 eV. One effect of temperature modulation is a broadening of the edge of the Fermi distribution function, producing an increase in ϵ_2 at low energies followed by a decrease in ϵ_2 at high energies.[18] Thus all three features are consistent with line shapes expected for interband transitions originating from, or terminating on, the Fermi surface. The 2.40-eV structure corresponds in energy to a feature seen in ϵ_2. The other features are near the shoulders seen on the low-energy side of the ϵ_2 structures labeled $E2$ and $E4$. The $\vec{k}$-space origin of structures in ϵ_2 and $\Delta\epsilon_2$ is discussed in the following section.

III. COMPUTATIONAL TECHNIQUES AND RESULTS

The self-consistent energy bands of NiAl shown in Fig. 3 were calculated using the augmented-

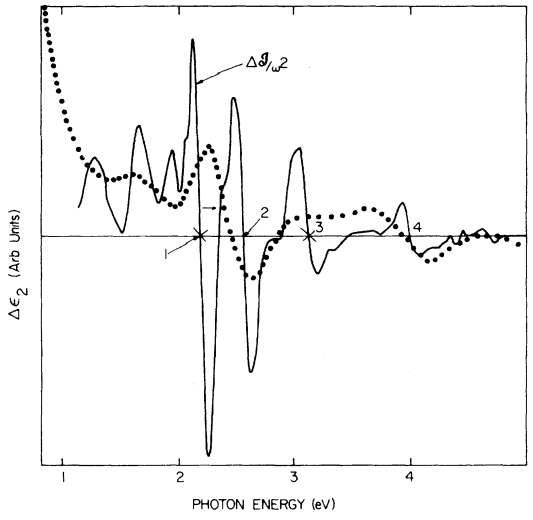

FIG. 2. $\Delta\epsilon_2(\omega)$ from thermoreflectance measurements (dotted line) and $\Delta\mathcal{J}(\omega)/\omega^2$ from JDOS calculations (solid line). Experimental evidence of transitions involving the Fermi surface is seen at 1.80, 2.40, and 3.95 eV. The $\vec{k}$-space origin of the numbered antisymmetric theoretical structures is summarized in Table II and discussed in relation to experimental features. The ×'s at zero crossings indicate transitions on symmetry lines not allowed by symmetry.

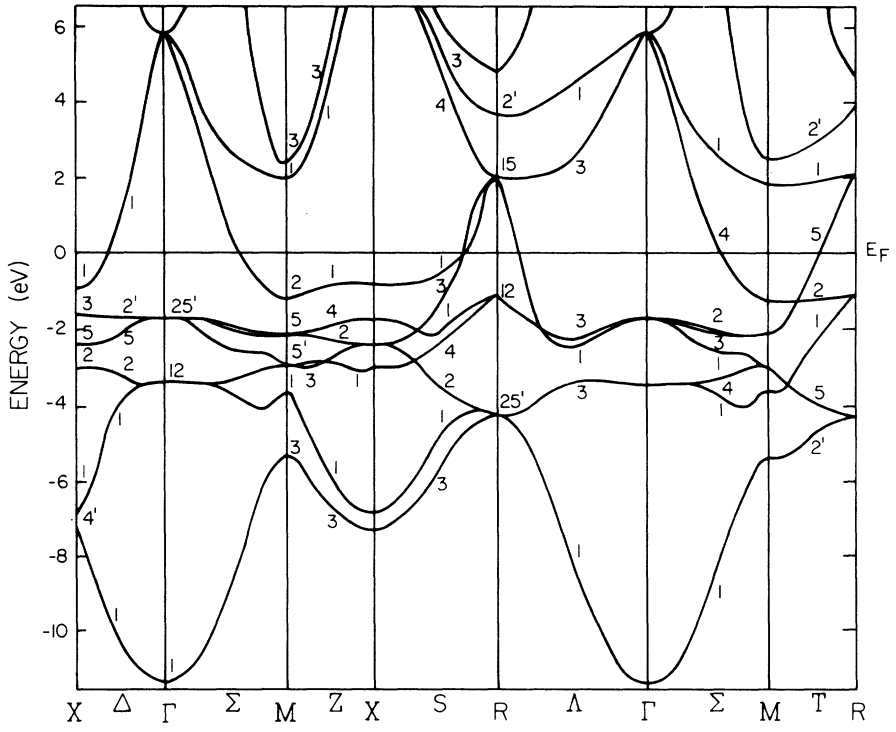

FIG. 3. Self-consistent energy bands of NiAl as calculated by Moruzzi, Williams, and Gelatt (Ref. 12).

spherical-wave method developed by Williams, Kübler, and Gelatt.[2] The results are in good agreement with older Korringa-Kohn-Rostoker NiAl calculations.[19] Energy eigenvalues at 363 points in the irreducible 1/48th of the Brillouin zone were least-squares fitted to 60 symmetrized plane waves with an average rms error of 2.6 mRy. These fits were then used to generate the band energies at the corners of 512 tetrahedra which filled the irreducible wedge of the Brillouin zone. Using the linear-energy tetrahedron method,[20] the density of states (DOS) and the joint density of states (JDOS) could then be calculated. For the JDOS, care was taken to include only the portion of the tetrahedron yielding empty final states or filled initial states when the Fermi surface intersected a tetrahedron.

If electric dipole matrix elements are approximately constant throughout the Brillouin zone, one may write

$$\epsilon_2(\omega) \propto |\langle \mathfrak{M} \rangle|^2 \mathcal{J}(\omega)/\omega^2 ,$$

where $\langle \mathfrak{M} \rangle$ is a matrix element and $\mathcal{J}$ is the JDOS. The solid line in Fig. 1 shows $\mathcal{J}(\omega)/\omega^2$, scaled with arbitrary units so that it can be compared easily to the experimental ϵ_2 spectrum. As can be seen, there is fairly good agreement between the gross features of the spectra. By calculating the JDOS, band-pair by band-pair, the origin of structure in $\mathcal{J}(\omega)$ is identified easily. Five features have been numbered in the curve of $\mathcal{J}(\omega)$ in Fig. 1. Their $\vec{k}$-space origins are summarized in Table I according to the nearest symmetry lines and band numbers (starting with the bottom band as number 1) involved. As indicated in the table, some of the transitions are not allowed along the symmetry

TABLE I. $\vec{k}$-space origin of features in the calculated function $\mathcal{J}(\omega)$ which are numbered in Fig. 1.

Structure number	1	2	3	4	5
Energy (eV)	2.06	2.20	2.56	3.06	4.35
Band of transitions	$6 \rightarrow 7$	$5 \rightarrow 7$	$4 \rightarrow 7$	$7 \rightarrow 8$	$2 \rightarrow 7$
Symmetry location	$\Sigma_2 \rightarrow \Sigma_4$	$\Sigma_3 \rightarrow \Sigma_4$	$T_1 \rightarrow T_5$	$T_2 \rightarrow T_1$	$\Sigma_1 \rightarrow \Sigma_4$
Symmetry allowed?	yes	no	yes	no	yes
Involves Fermi surface?	yes	yes	yes	no	no

TABLE II. $\vec{k}$-space origin of features in the calculated function $\Delta\mathcal{J}(\omega)$ which are numbered in Fig. 2.

Structure number	1	2	3	4
Energy (eV)	2.18	2.54	3.09	4.00
Band of transition	$5 \rightarrow 7$	$4 \rightarrow 7$	$3 \rightarrow 7$	varies
Symmetry location	$\Sigma_3 \rightarrow \Sigma_4$	$T_1 \rightarrow T_5$	$\Delta_1 \rightarrow \Delta_2$ $\Sigma_4 \rightarrow \Sigma_4$	many
Symmetry allowed?	no	yes	no yes	yes
Seen in $\mathcal{J}(\omega)$?	yes	yes	yes	no

lines. In particular, features 2 and 4 are due largely to transitions near $\Sigma_3 \rightarrow \Sigma_4$ and $T_2 \rightarrow T_1$ which, along these symmetry lines, are not allowed. Thus, especially for structure 4, where the lines T_2 and T_1 are quite parallel near $\mathfrak{M}$, with matrix elements taken into account, these two structures shrink and broaden into better agreement with experiment. We now re-examine the thermoreflectance results using similar computational techniques.

If we assume that matrix element variation with temperature is negligible we may write

$$\Delta\epsilon_2(\omega) \propto |\langle \mathfrak{M} \rangle|^2 \Delta\mathcal{J}(\omega)/\omega^2.$$

Structure in $\Delta\epsilon_2$ can thus be related to regions in the Brillouin zone where the temperature dependence of the JDOS is large. This may arise via the effect of thermal expansion on band gaps, via phonon broadening, and, in metals, when interband transitions involve the Fermi surface, via the temperature dependence of the Fermi function.[17] When present, the latter gives large thermomodulation spectral features. The effect of a change in E_F/kT can be examined by evaluating

$$\Delta\mathcal{J}(\omega) \equiv \tfrac{1}{2}[\mathcal{J}(\omega, E_F - \delta) + \mathcal{J}(\omega, E_F + \delta)] - \mathcal{J}(\omega, E_F),$$

where, as before, $\mathcal{J}$ represents the JDOS. This function, calculated with $\delta = 10$ mRy and scaled by ω^2, is shown in Fig. 2 as a solid line for comparison with $\Delta\epsilon_2$. It represents, in arbitrary units, $\Delta\epsilon_2$ arising from an increase in temperature. As can be seen, there is a great deal of structure in this type of computed spectrum which, due to matrix element effects and broadening, is not seen experimentally. Furthermore, no theoretical modulated Drude term was added. However, such calculations are quite beneficial in identifying structure in the thermoreflectance data. Four structures in Fig. 2 are numbered and their $\vec{k}$-space origins summarized in Table II. As can be seen by comparing Tables I and II, the first three $\Delta\mathcal{J}$ structures are close to structures seen in $\mathcal{J}$ although the $\vec{k}$-space origin for the third is much different. The structure in $\Delta\mathcal{J}$ at 4.00 eV involves many different regions in $\vec{k}$ space and, though no distinct feature is seen in $\mathcal{J}$ at this energy, the shoulder on the low-energy side of the broad peak labeled $E4$ in Fig. 1 is due to these transitions.

One must be cautious in comparing Figs. 1 and 2. Modulation of the Fermi function for transitions beginning or ending at the Fermi level results in spectra with positive and negative peaks whose zero crossings do *not* occur at the maxima of the corresponding structure in ϵ_2. For transitions from a narrow band of initial states to the Fermi level the zero crossing is at threshold, while if the initial states occur over a range in energy, the zero crossing shifts to an energy higher than the threshold for the transitions, the shift depending on the electric dipole matrix elements and the density of initial states. The energy dependence of the density of final states plays a negligible role in the thermomodulation spectra for such transitions, but it is important in ϵ_2, and plays a role in locating peaks. Similar arguments apply for transitions originating at the Fermi level. Thus the transitions dominating $\Delta\epsilon_2$ may not contribute much to ϵ_2, and the features related to excitations to or from the Fermi energy contribute significantly to $\Delta\epsilon_2$ but sometimes appear only as thresholds in ϵ_2, not as peaks.

We now conclude this section by identifying the structure seen in the optical experiments with features in the calculations, acknowledging that in some cases, matrix elements would be desirable. This interpretation is summarized in Figs. 1 and 2, where lines are drawn connecting features in the computed curves with those in the experimental spectra. The $\times$'s denote calculated transitions which are forbidden on the symmetry lines (see Tables I and II). The gross structure, labeled $E2$ in Fig. 1, is due primarily to transitions originating about 2.5 eV below E_F. The structure labeled $E4$ does not involve the Fermi surface except for the shoulder on the low-energy side. Self-energy corrections can lead to energy corrections of the order of 10%.[19] Thus, taking symmetry considerations into account, the JDOS appears to be quite accurate. In Fig. 2, it appears that the structure in $\Delta\epsilon_2$ at 2.40 eV is due to a sum of $\Delta\mathcal{J}$ contribu-

tions 1 and 2. This is a case where matrix elements are needed; however, this identification appears to fit well with the same identification in Fig. 1. Again, rather good agreement is obtained between $\Delta\epsilon_2$ and $\Delta\mathcal{J}$.

IV. CONCLUSIONS

Our identification of the $\vec{k}$-space origin of states giving rise to the large broad peak labeled E2 in Fig. 1 shows that the transitions involved are primarily from below E_F to E_F. This is at odds with the previously published interpretations, even those involving the use of band-structure calculations, which were that the transitions were from states at the Fermi energy to states above it. Connolly and Johnson carried out a non-self-consistent augmented-plane-wave calculation, computing a DOS, JDOS, and indirect JDOS.[11] Noting the similarity of the JDOS and indirect JDOS, they ascribed the optical features in ϵ_2 to structure in the DOS. In their DOS calculations (as in ours) the product of the DOS 2.5 eV below E_F and that at E_F is many times greater than the product of the DOS at E_F and that at 2.5 eV above E_F. Nevertheless, they assign the 2.5-eV peak (actually 2.1 eV in their calculation) to transitions from E_F to states above, thus agreeing with previous experimental interpretations. In their charge analysis they found the DOS at E_F to be composed primarily of Al s and p functions and appealed to the rigid-band model to argue that, on the Ni-rich side of stoichiometry (where Ni substitutes for Al), as Al decreases, E_F decreases. One would then expect that if, as they asserted, the $E2$ structure were due to transitions from E_F to states above, as E_F decreased the threshold energy for these transitions would increase. They then pointed to the change in energy of the $E1$ minimum, seen in the early experiments of Jacobi and Stahl,[7] to confirm this behavior. They further suggested that the previously reported optical results for CoAl,[3] in which the 2.5-eV peak was absent, provided further evidence that filled initial states near E_F in NiAl were responsible for the $E2$ structure and that these states were completely empty in CoAl. Jacobi and Stahl,[21] in later work with ternary alloys including Ni and Al, did not see the definite $E1$ minimum that they had seen in their earlier work, cited by Connolly and Johnson. In fact, their results suggest that the energy position of this minimum in ϵ_2 should not be taken as a threshold for transitions contributing to the $E2$ structure. Jacobi and Stahl did conclude that the concentration-dependent optical properties, including the peak height and peak position of the $E2$ structure, could be understood using the rigid-band model. They suggested that the $E2$ structure was due to parallel-band absorption at R with transitions originating at E_F and they interpreted Nilsson's photoemission results as confirming their assignment.[21] Although Nilsson did not address the origin of the 2.5-eV peak, his discussion can only be taken as contradicting the assignments of Jacobi and Stahl.[22] Nilsson claimed that his results supported the DOS (and therefore the energy bands) of Connolly and Johnson.[11] In these bands, the closest occupied states to E_F at R were almost 1 eV below E_F. In affirming our interpretation, the previous optical measurements, especially of CoAl, and the use of the rigid-band model need to be examined.

The CoAl measurements referred to by Connolly and Johnson and other more recently reported results do not, in fact, lack the 2.5-eV structure. We assert, rather, that it is shifted to lower energy and is masked both by additional interband transitions and possibly by a large Drude contribution. In Fig. 4 we show $\mathcal{J}(\omega)/\omega^2$ using the NiAl bands but a CoAl Fermi level. As can be seen, the $E4$ structure remains but is quite small relative to the low-energy features. The 2.5-eV structure is not discernable as a peak simply because other transitions are now allowed. It is not until about 0.8 eV that the interband transitions turn off and at this energy the Drude term may be too large to detect the strong onset. Comparison of the NiAl bands with self-consistent CoAl bands[23] shows that transitions contributing to the $E2$ structure ($\Sigma_2 \rightarrow \Sigma_4$ and $T_1 \rightarrow T_5$—see Table I) shift to lower energy by about 0.5 eV. In the experiments cited by Connolly and Johnson, the low-energy limit was 1.75 eV[3]. The results of Kiewet and Brittain,[23] whose experiments had a 0.7-eV limit,

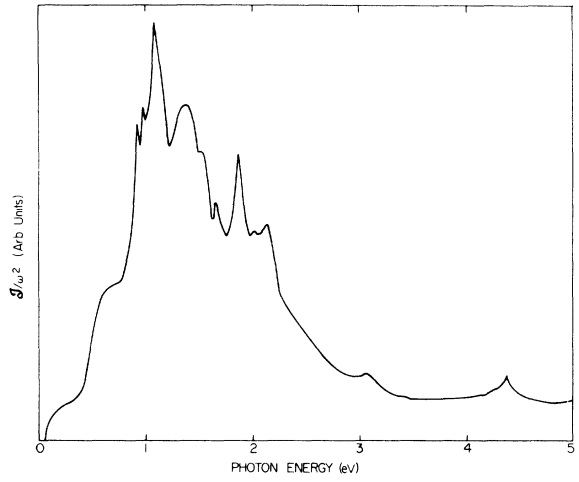

FIG. 4. $\mathcal{J}(\omega)/\omega^2$ from JDOS calculations of CoAl using the NiAl energy bands of Fig. 3.

are consistent with Fig. 4, in that optical structure is seen at low energy and the value of ϵ_2 at 1.5 eV is much greater than at 4 eV. Furthermore, they were not able to obtain a good Drude fit to the CoAl spectrum while they could for that of NiAl, indicating the importance of low-energy interband transitions in CoAl.

Many different experiments on β'-NiAl and similar systems have been employed in attempts to understand the changes in electronic structure with changes in concentration. The large changes in optical peak heights seen also in ternary compounds, are still quite puzzling. Claims that changes in peak height and position follow rigid-band behavior are unjustified in two respects. First, the movement of peak position is not necessarily indicative of a change in the Fermi level. As discussed earlier, one needs an experiment such as thermoreflectance to monitor the Fermi level since it is thresholds, not peaks, that are important. Second, even if a rigid-band model were to explain shifts in thresholds adequately, changes in peak amplitude are much more difficult to predict. Changes in the bands bring changes in hybridization that may be important in understanding the peak height variation through the effect of dipole matrix elements. Our results lend strong support to the details contained within the self-consistent energy bands of Moruzzi, Williams, and Gelatt. The character of these bands, when compared with that of the CoAl energy bands,[24] indeed indicates that a rather severe change in DOS from all but the d-like states occurs. In any case, the rigid-band model cannot be used to identify the 2.5-eV peak as arising from transitions originating from E_F.

How then can these alloys be understood? Several additional experiments and calculations would be helpful. Optical reflectance at low energy should confirm the above assertions about the electronic structure of CoAl. Thermoreflectance experiments monitoring the Fermi level as a function of composition would lead to a more meaningful interpretation of the reflectance results. More sophisticated calculational techniques such as the coherent potential or renormalized atom approximations, which could more specifically investigate concentration effects, would be illuminating and could perhaps demonstrate the importance of changes in hybridization.

ACKNOWLEDGMENTS

This work was supported in part by the U.S. Department of Energy, Contract No. W-7405-Eng-82, Division of Materials Sciences, Budget Code No. AK-01-02-02-2 and by NATO Research Grant No. 1150. We wish to thank F. A. Schmidt of the Ames Laboratory for the preparation of the alloys.

*Present address: Istituto di Fisica 'G. Marconi', Università di Roma, 00185 Rome, Italy.

[1]O. K. Andersen, Phys. Rev. B 12, 3060 (1975).
[2]A. R. Williams, J. Kübler, and C. D. Gelatt, Jr., Phys. Rev. B 19, 6094 (1979).
[3]T. Sambongi, R. Hagiwara, and T. Yamadaya, J. Phys. Soc. Jpn. 21, 923 (1966).
[4]D. A. Kiewit, J. J. Rechtien, and J. O. Brittain, J. Phys. Soc. Jpn. 21, 2380 (1966).
[5]J. J. Rechtien, C. R. Kannewurf, and J. O. Brittain, J. Appl. Phys. 38, 3045 (1967).
[6]H. Jacobi, B. Vassos, and H. J. Engell, J. Phys. Chem. Solids 30, 1261 (1969).
[7]H. Jacobi and R. Stahl, Z. Metallkde. 60, 106 (1969).
[8]Y. Yamaguchi, T. Aoki, and J. O. Brittain, J. Phys. Chem. Solids 31, 1325 (1970).
[9]K. Adachi, T. Katayama, and T. Hirone (unpublished) (See Ref. 8).
[10]K. H. Johnson and J. W. D. Connolly, Int. J. Quantum Chem. IIIS, 813 (1970).
[11]J. W. D. Connolly and K. H. Johnson, Nat. Bur. Stand. (U. S.) Spec. Publ. 323, 19 (1971).
[12]V. L. Moruzzi, A. R. Williams, and C. D. Gelatt, private communication.
[13]L. W. Bos and D. W. Lynch, Phys. Rev. B 2, 4567 (1970).
[14]T. J. Moravec, J. C. Rife, and R. N. Dexter, Phys. Rev. B 13, 3297 (1976).
[15]H. J. Hagemann, W. Gudat, and C. Kunz, Solid State Commun. 15, 655 (1974); Phys. Status Solidi B 74, 507 (1976).
[16]R. Rosei and D. W. Lynch, Phys. Rev. B 5, 3883 (1972).
[17]A. Balzarotti, E. Colavita, S. Gentile, and R. Rosei, Appl. Opt. 14, 2412 (1975).
[18]M. Cardona, *Modulation Spectroscopy*, Solid State Physics, edited by F. Seitz, D. Turnbull, and H. Ehrenreich (Academic, New York, 1969), Suppl. 11, pp. 130–136.
[19]V. L. Moruzzi, A. R. Williams, and J. F. Janak, Phys. Rev. B 10, 4856 (1974).
[20]O. Jepsen and O. K. Anderson, Solid State Commun. 9, 1763 (1971); G. Lehmann and M. Taut, Phys. Status Solidi B 54, 469 (1972).
[21]H. Jacobi and R. Stahl, J. Phys. Chem. Solids 34, 1737 (1973).
[22]P. O. Nilsson, Phys. Status Solidi 41, 317 (1970).
[23]D. A. Kiewit and J. O. Brittain, J. Appl. Phys. 41, 710 (1970).
[24]D. J. Nagel, L. L. Boyer, D. A. Papaconstantopoulos, and B. M. Klein, in *Transition Metals, 1979*, edited by M. J. G. Lee, J. M. Perz, and E. Fawcett (Institute of Physics, Bristol, 1979), p. 104.